Provision of frequency support by offshore wind farms connected via HVDC links

A.B. Attya*, O. Anaya-Lara*

**Department of Electronic and Electrical Engineering, University of Strathclyde, Glasgow, UK*
Corresponding author email: ayman.attya@strath.ac.uk

Keywords: wind power, power systems, ancillary services, HVDC, energy storage

Abstract

The high penetration levels of wind power will obligate wind farms to contribute to the mitigation of frequency drops. Comprehensive case studies are presented to investigate the different methods of frequency support provision by wind power. The implemented test system is composed of an offshore wind farm connected to an external grid through a point-to-point HVDC link. Three different frequency support methods are compared; droop de-loading, battery storage banks and a mix between the two methods. Moreover, two different methods of sensing the frequency drop, at the point of common coupling, by the wind farm are examined. The impact of the HVDC is highlighted, especially its role to transmit the power surge provided by the wind farm. A modified de-loading controller is developed and integrated to all the wind turbines, according to the executed case studies. Results show that the proposed frequency support solutions have almost similar impact on the natural frequency response at the point of common coupling. The HVDC link does not worsen the frequency response, and the fluctuations in voltage levels at onshore and offshore buses are very minor. DIGsILENT PowerFactory is integrated as a simulation environment.

1 Introduction

The replacement of conventional (i.e. synchronous generators) with renewable energy sources interfaced by power electronics (PE) converters will reduce the system overall inertia making it more vulnerable to frequency excursions [1]. As an illustration, the PE converters which couple the renewable energy conversion systems (e.g. wind) screen the frequency variations of power system due to the fast responsive PE interface. Hence, wind power, with stored kinetic energy, will not respond naturally to frequency excursions (i.e. inertia response). In addition, the dispersion of generation (i.e. Large synchronous plants will be replaced with hundreds of wind turbine generators (WTGs) spreading over several kilometres) will also affect the power system inertia. The system inertia plays a key role during the early stage of the frequency drop as it mitigates frequency deterioration beyond a certain threshold (absolute deviation or *frequency nadir*) to avoid load shedding. The theory of frequency support by wind farms (WFs) is based on the endowment of an active power surge during the frequency drop to mitigate the generation-demand unbalance as a main cause to frequency deviations. Securing stable energy resources and managing this power surge are the main challenges facing the provision of this ancillary service by wind power. In particular, there are two types of frequency support which could be provided by WTGs, namely the inertia response and primary response [2]. The two types of frequency regulation can be achieved by the extraction of certain amount of kinetic energy (KE) stored in the rotating parts of the WTG. This KE is depleted to increase the electrical output, then the speed stabilizes at a new slower speed. However, this method requires a recovery period after the frequency drop is eliminated such that the WTG restores its normal speed [3]. The second method depends on *de-loading*; operating the WTG to provide output power less than the available (i.e. Maximum Power Tracing (MPT) is violated). De-loading has two types; Delta and Balance; at *Delta* the output power is reduced by a certain *percentage* of the available power, meanwhile in *Balance* mode the output is reduced by an *absolute value* (e.g. 0.2 per unit) [4]. The dominant de-loading ratio (Delta mode) ranges from 10% to 20% of the available wind power [5], where the average wind speed, rating of WTG, and the expected level of frequency support are the main deciding parameters. The previous methods count only on the available wind power just before, during and shortly after the frequency event. Hence, these methods are vulnerable to wind speed changes and their contribution to frequency support is changing from one event to another. In addition, it makes the WTG deviates from MPT most of the time, which implies negative economic impact on the wind farm's owners. The solution to overcome these obstacles is to depend on an alternative, more stable and highly predictable source of energy to provide the required power surge. Literature had investigated several types of energy storage systems, some of them are still in very early stage of research and prototyping, and others stand on a solid ground of mature technologies [6]. In this paper, batteries' banks are in focus as they are widely applied in power systems and extensively examined in the literature.

This paper investigates the capability of an offshore wind farm (WF), which is connected via a point-to-point HVDC link to provide frequency support. Three methods are examined; drooped de-loading, energy storage and a mix between both. A simplified method is applied to estimate the de-loading ratios and battery bank rated power so that the power surges that are provided in all cases are almost the same. The role played by the PE converters of the HVDC link will be considered and the impact on the voltage stability at

onshore and offshore buses is analysed. The paper is composed of five sections including this introduction. The next section describes the implemented benchmark, and Section 3 explains the applied case studies. Results are presented and discussed in Section 4, finally fifth section concludes.

2 Implemented benchmark system

The implemented system is composed from an offshore wind farm of 400 MW installed capacity (80 x 5 MW Double Fed Induction Generators; DFIGs) which is connected to the external grid through a bi-pole HVDC link (100 km with 150 kV rated voltage, and transfer capacity of 450 MW). The HVDC is controlled using a Voltage Source Converter (VSC) that controls the offshore voltage and frequency through six pulse converters. The system single line diagram is shown in Figure 1 (a clearer figure for the controller is shown later in Figure 5), meanwhile the system model in DIGsILENT PowerFactory is displayed in Figure 2. The WF generation is collected through five feeders; each feeder is connecting a ring of WTGs. Three feeders each connects a ring of 20 WTGs, while the fourth and fifth each connects a ring of 10 WTGs. The WTGs connected through the same ring (i.e. to the same main feeder) are modelled as an aggregate one WTG with an equivalent installed capacity (e.g. First ring with 20*5 MW installed capacity). However, the WTGs connected to the fifth ring are simulated as 10 different models to provide more detailed results. The WF layout is shown in Figure 3. The WTG model is detailed to include the turbine, shaft, PQ controls of converters, and protection devices. These models are already embedded in the DIGsILENT 5MW-DFIG template, and the default values of the parameters are applied. Likewise, the HVDC link detailed model is integrated using the embedded model in DIGsILENT library. The External grid model is used with a 10 GVA short circuit capacity and acceleration factor of 8 s, and it is considered as a slack bus. The short circuit ratio with respect to WF capacity is 25 which is an average strength grid moderately resistible to frequency deviations [7]. Measurement issues caused by the Phase-Locked loop (PLL), which is used to measure frequency, are considered. A typical model of PLL (Embedded in DIGsILENT library) is integrated with proportional and integral gains of 10 and 1 respectively, and the measurements at the point of common coupling (PCC).

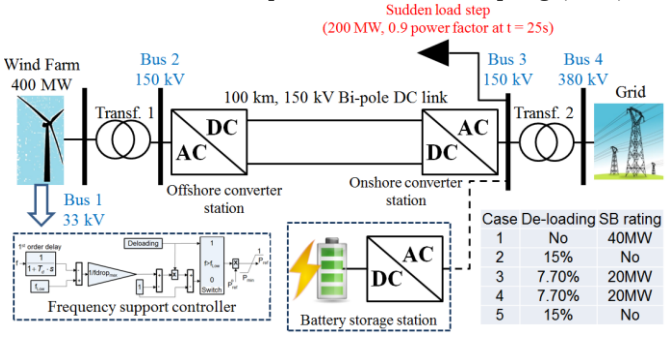

Figure 1 Implemented benchmark system

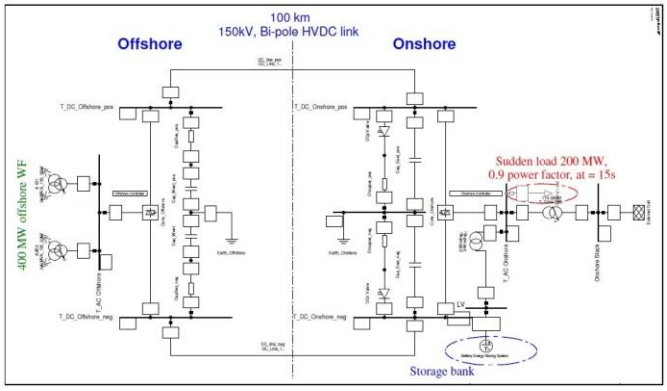

Figure 2 Benchmark system actual model in DIGsILENT

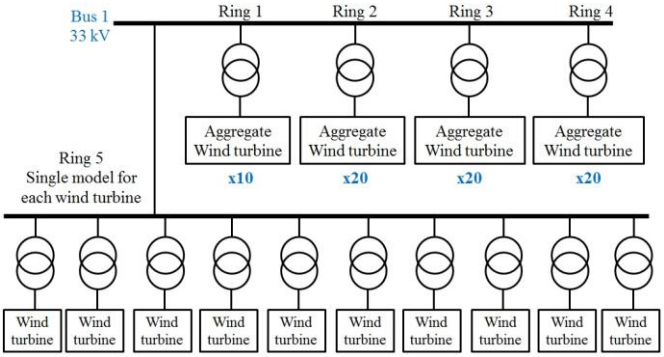

Figure 3 Wind farm layout as modelled in DIGsILENT

3 Case studies

The implemented case studies investigate the impact of the WF integration on the natural (i.e. Inertia) frequency response at a moderate drop. The frequency drop is generated through a sudden load step increase (200 MW, 0.9 power factor) at the onshore AC low voltage bus (Bus 3; PCC). In all the case studies, the external grid doesn't provide primary or secondary response to highlight the impact of WF contribution to the unregulated frequency recovery. The WF production is fixed to an average value of 250MW. In the *base case* the WF is integrated but it does *not* provide any frequency support.

3.1 Case 1: battery storage integration

A battery storage bank (SB) of 40 MW (10% from the WF installed capacity) is integrated at the onshore Bus 3 as shown in Figure 1. The assumed size of the SB is inspired from the literature recommendations and previous studies [8]. The SB is controlled to charge when the frequency deviation exceeds certain positive threshold (50 mHz), and discharge with 0.004 pu/1Hz drop (i.e. Provide power surge) to mitigate the frequency drop as shown in Figure 4. This specific droop value is selected to ensure that the SB will provide its rated power to mitigate the frequency drop. The SB is central, in other words, no SB is connected to each WTG, but a central storage station is connected to the network at the PCC.

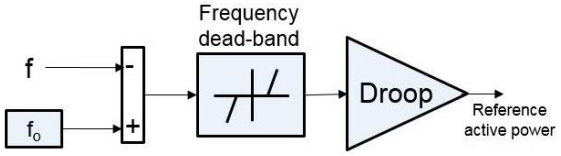

Figure 4 SB frequency support supplementary controller

The onshore location of the SB is selected for the following reasons:

- To curtail the installation and maintenance costs, as they are higher for offshore.
- SB power is not delivered via the HVDC link to simplify the control methods, and reduce transmission losses, as well as the HVDC link required capacity.
- It is closer to PCC, hence clearer impact on frequency deviations, and the required measurements and communications are simpler.
- Batteries could be charged from the grid or the WF, however, this point is out of the scope of this study.

3.2 Case 2 Droop control only

A supplementary controller is integrated into the WTG. This controller receives the frequency measurement signal (f) at the onshore Bus 3, and the nominal reference power (P^o_{ref}) as input signals. The output is a rescaled value for the reference power signal fed to the PQ controller of the WTG converter as shown in Figure 5. The expected delay caused by communicating frequency measurements is interpreted by a 10ms first order delay. The controller de-loads the reference power signal nominal value (highest possible power, according to MPT; P^o_{ref}) by a certain Deloading factor when there is no frequency deviation (i.e. deviation is better than -50 mHz; at nominal frequency (fo) = 50 Hz, hence fLow = 49.95 Hz. The violation of frequency threshold initiates a ramp increase in the reference power, such that the nominal value is retained when the deviation reaches a predetermined value, namely $fdrop_{max}$ (0.2 Hz in this paper).

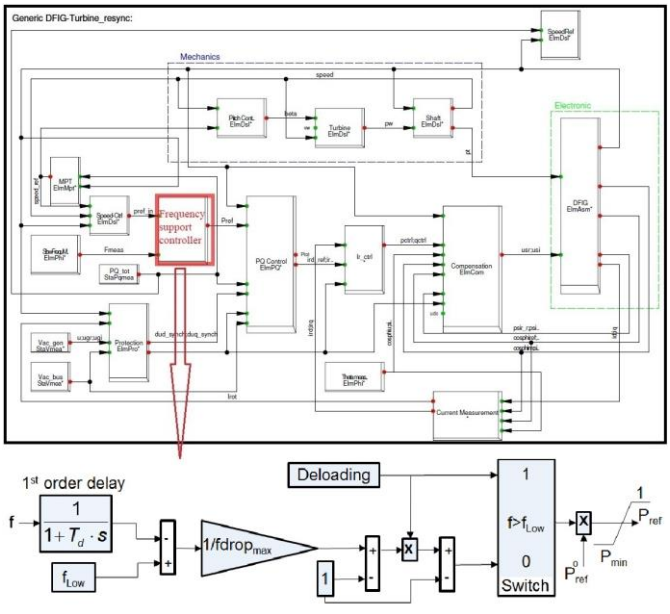

Figure 5 Integrated frequency support controller

This support method could be considered of Delta type as previously explained. It is of note that, during de-loading operation P_{ref} has a minimum limit to maintain a reasonable WTG output at low wind speed conditions. In addition, a maximum limit is applied, namely 1 per unit to avoid the overloading of the WTG generator.

3.3 Case 3 Merging between droop support and storage

Both SB and the droop controller are integrate. However, the de-loading ratio and the SB size are reduced. The amount of reduction is decided based on the maximum available power surge from each method. In particular, at an average wind speed, and a de-loading ratio of 15%, the integrated WTG can provide about 0.093 per unit (0.46 MW), thus for the whole WF 0.46*80 = 36.8 MW. On the other hand, the SB can provide its rated power, namely, 40 MW. The average value is selected as an expected aggregate power surge from both sources in Case 3, namely 38.4 MW. The WF should contribute by 38.4*0.5 MW (i.e. the required power step is equally shared between the WF and the SB), thus the de-loading ratio and the SB rated power are approximately 7.7% and 20 MW respectively.

3.4 Case 4 Follow SB response

The WF provides the support by following the response of the SB. The supplementary controller in Figure 5 is modified to follow the output power of the SB as shown in Figure 6. The elimination of Δf signal avoids the challenges caused by PLLs and simplifies the nature of the communicated data. The output power of the SB is measured using a Phase Measurement Unit (PMU [9]) at the point of connection. The de-loading is removed proportionally to the per unit output power of the SB (i.e. *no* de-loading at the rated output of the SB). In this case, the controller in the WTG is only responsible to de-load the WTG as long as the SB output is zero (i.e. no frequency event). When a frequency drop occurs, the frequency dead-band and the droop ratio of the SB controller drive both the SB output, and the removal of WTG de-loading. The SB rated power and WTG de-loading ratio in Case 3 are applied in this case study.

3.5 Case 5 Voltage-Frequency lookup table

This case is similar to Case 2 except the integration of a novel approach to eliminate the need for frequency measurements. The main perspective is to replace the PLL with a PMU (to monitor the voltage at the PCC). The voltage deviation at PCC is analysed in correspondence to the frequency deviation. Thereupon, the required data to have a single dimensioned lookup table is obtained. The input to this table will be the incident voltage deviation in per unit, and the output is the estimated frequency deviation also in per unit. The expected errors in frequency deviation estimation are expected to affect the provided frequency support very slightly. The impact might have an influence at low frequency deviations (i.e. when the frequency deviation is below the threshold that triggers the full frequency support, for example $fdrop_{max}$ in the proposed de-loaded support method).

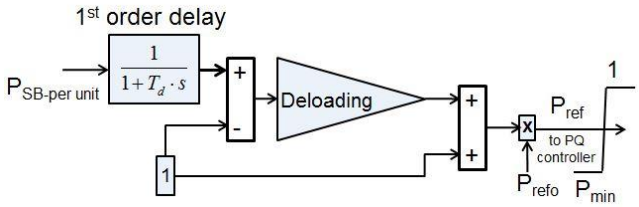

Figure 6 SB follower frequency support controller

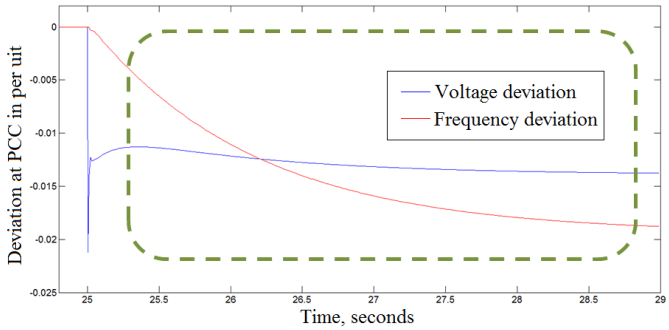

Figure 7 Integrated frequency support controller

The interval of very fast drop in voltage, at the initial moments of the frequency drop, is eliminated. In addition, the interval through which the voltage rises and then drops again is also rejected. Thus the extracted data fit with linear interpolated lookup tables. An example for the data used to obtain the lookup table is shown in Figure 7 based on the examined base case. The lookup table is set to assure zero output when the voltage deviation is positive or zero. The applied case SB ratings and de-loading ratios in all the examined case studies are shown in Figure 1.

4 Results and discussion

The frequency response is improved in all cases compared to base case due to the provision of frequency support by the SB and/or the WF. The initial rate of change of frequency (RoCoF) is improved and the frequency nadir is mitigated as shown in Figures 8-a and 9. The frequency responses of all cases are almost identical which ensures the feasibility and the similarity between the investigated methods to provide frequency support (i.e. SB, WF de-loading and both) with three different sensing methods (PLL measurements, SB follow and voltage-frequency lookup table). In addition, the simple algorithm applied in Case 3 to resize the SB, and set the de-loading ratio leads to the same response caused by each method independently. The average values of RoCoF, during the first 500ms after the event, is not violating the widely applied threshold, namely, 1 Hz/s [10], in all cases as shown in Figure 9. The highest improvement occurred when the WF follows the SB response the improvement in RoCoF is mitigated. This mainly returns to the selected control parameters of the SB. The voltage – frequency deviation lookup table has slightly hindered the RoCoF improvement. This returns to the slower voltage deterioration compared to the frequency deviation. This could be treated through developing the applied method to obtain the data of the lookup table.

4.2 Voltage response

The focus of this study is on the supportive active power and frequency stability; however it is important to check that the voltage deviations at major buses are not violating normal operation limits. In Figure 8, the voltage of the offshore Bus 2 is slightly affected (i.e. about 0.01 per unit drop), especially in Case 2 when the full support is provided by the WF due to the higher power surge (i.e. higher de-loading compared to other cases where the WF is contributing to frequency support). Conversely, the voltage is fixed through the frequency event in Base case and Case 1 because the HVDC link blocks the frequency variations occurring at the onshore side. The external grid bus (Bus 4) is more affected where the deviation reached 0.02 per unit in Base case, and then improved to 0.017 per unit in the other cases.

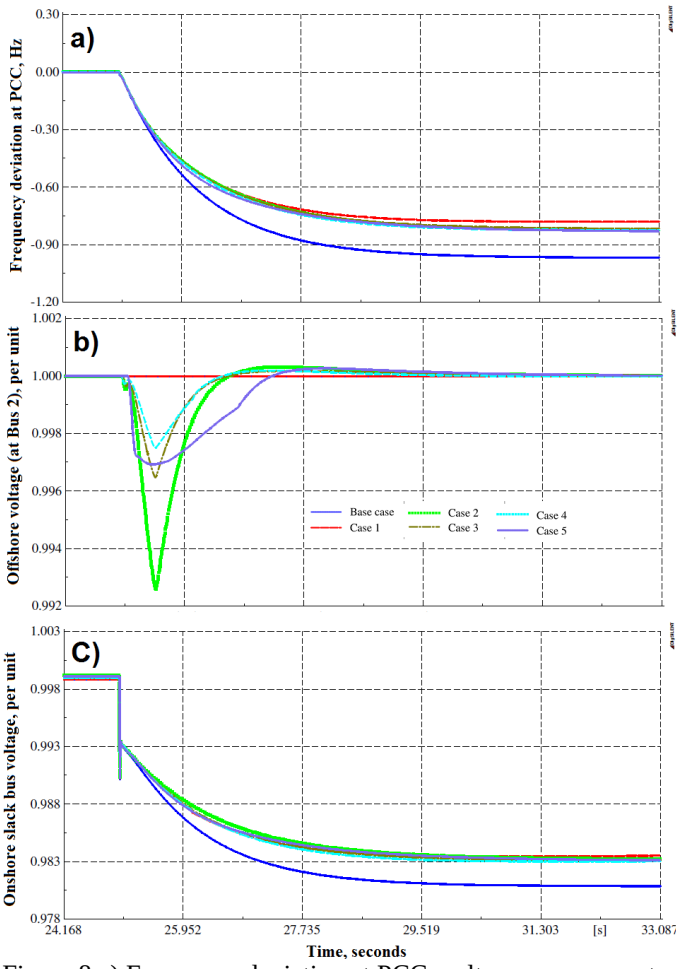

Figure 8 a) Frequency deviation at PCC, voltage responses at b) Bus 2 and c) PCC

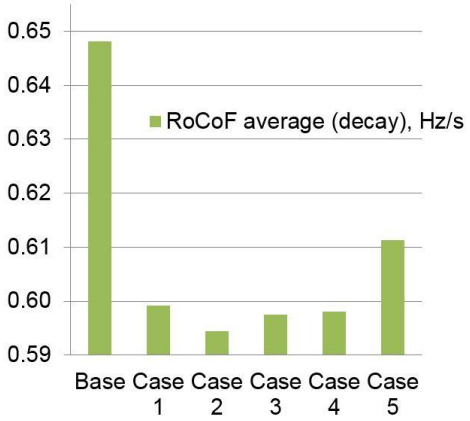

Figure 9 Decaying RoCoF during the first 500ms of the event

4.3 Power delivery

The power surge provided by the SB is relatively more fixed as shown in Figure 10-a. As an illustration, the inertia of the WTG and the limits imposed on the rate of change of power (+/- 0.5 per unit) make the power surge requires a few seconds until it stabilizes at the nominal output (i.e. not de-loaded). The installation of the SB at the onshore bus (Bus 3) cancels any influence for the HVDC, hence the responses of the delivered power via the HVDC in Base case and Case 1 are identical. The power surge of the SB reaches its steady state value faster than the WTG (i.e. this is considered as a synthetic inertial response).

The power surge provided by the WF is delivered smoothly and with almost no delay through the HVDC as shown in Figure 10-b. As soon as the frequency drop is initiated, the HVDC link controllers change the set-point of the delivered power to maintain the new amount of power generated by the WF. It is of note, the perfect match between the overall responses of the aggregate WTG and that of the HVDC link as shown in Figure 10-c. The power delivered through the HVDC link is evenly distributed between the two poles so that the full capacity of the link is always available.

The applied method to provide and sense the frequency event proved to have a clear impact on the behaviour of the provided power surge by the WF. The fastest rising rate of the WF is recorded in Case 4, when the WF follows the SB. In contrast, the slowest rise occurs when the voltage – frequency deviation lookup table is integrated.

5 Conclusions

Two different methods are investigated to make the offshore wind farm, which is connected via an HVDC link, to participate directly or indirectly in frequency support. These methods are based on the provision of a fast power surge as soon as the frequency deviation violates certain margin. The source of this power could be the difference between the de-loaded and nominal outputs of the wind farm or the discharging power from a storage bank or both.

Results revealed that as long as the amount and speed of response of the provided surge power is unchanged (Regardless the applied method to obtain this surge) the frequency response at the point of common coupling is the same. A simple compromise is proposed to merge between the de-loading method and the integration of storage bank. Thus, the rated power of the storage bank is reduced (i.e. cost is mitigated), and de-loading ratio is also reduced, hence the wasted wind energy due to de-loading is curtailed.

The sensing of the frequency event by the wind farm is executed through three different methods. Conventional PLL proved to be sufficient to provide satisfactory response, while the concept of voltage-frequency lookup table slightly slows the building up of the power surge. The simplest method is to make the wind farm follow the response of the onshore storage bank.

Further case studies can integrate a conventional running reserve near the point of common coupling to compare its primary and secondary (i.e. Automatic Generation Control) responses with/without the proposed frequency support methods. In addition, the case of an island system could be examined to discover the main alteration in frequency response between an average strength grid and an isolated power system.

Acknowledgements

This work is partially supported by the EU FP7 project IRPWind. Grant agreement Number: 609795.

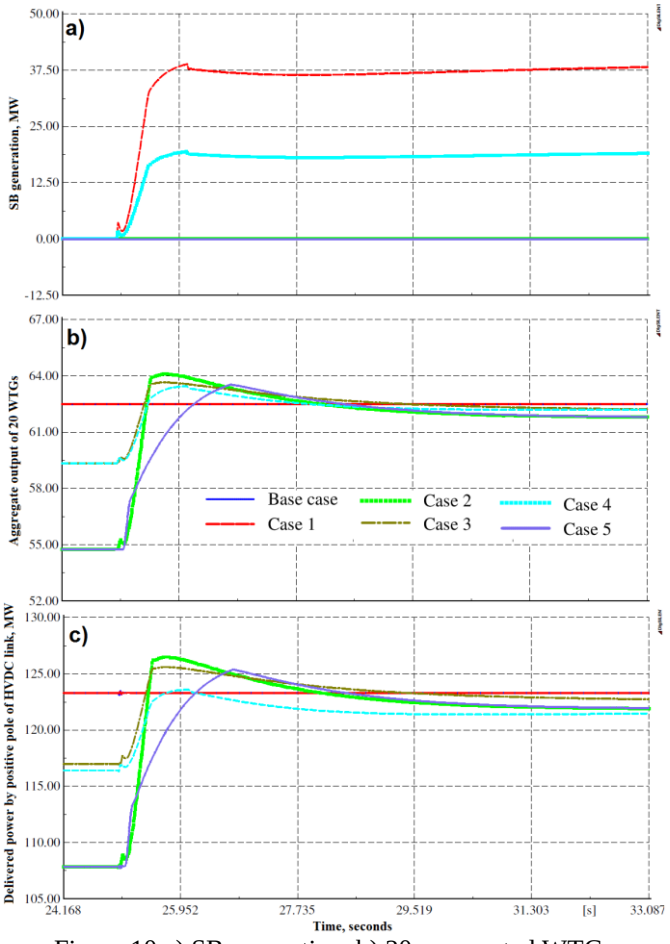

Figure 10 a) SB generation, b) 20 aggregated WTGs generation, and c) delivered power by the HVDC link

References

[1] S. El Itani, U. D. Annakkage, and G. Joos, "Short-term frequency support utilizing inertial response of DFIG wind turbines," in Power and Energy Society General Meeting, 2011 IEEE, 2011, pp. 1-8.
[2] A. B. Attya and T. Hartkopf, "Wind turbine contribution in frequency drop mitigation - modified operation and estimating released supportive energy," IET Generation Transmission & Distribution, vol. 8, pp. 862-872, May 2014.
[3] A. B. T. Attya and T. Hartkopf, "Control and quantification of kinetic energy released by wind farms during power system frequency drops," IET Renewable Power Generation, vol. 7, pp. 210-224, May 2013.
[4] I. D. Margaris, S. A. Papathanassiou, N. D. Hatziargyriou, A. D. Hansen, and P. Sorensen, "Frequency Control in Autonomous Power Systems With High Wind Power Penetration," IEEE Transactions on Sustainable Energy, vol. 3, pp. CP2-199, Apr 2012.
[5] M. Bhuiyan and S. Dinakar, "Comparing and Evaluating Frequency Response characteristics of Conventional Power Plant with Wind Power Plant," Master Thesis, Chalmers University of Technology, Goteborg, 2008.
[6] Juan A. Martinez, "Modeling and Characterization of Energy Storage Devices," presented at the IEEE Power and Energy Society General Meeting, Detroit Michigan, 2011.
[7] C. Li-Jun and I. Erlich, "Doubly Fed Induction Generator Controller Design for the Stable Operation in Weak Grids," IEEE Transactions on Sustainable Energy, vol. 6, pp. 1078-1084, 2015.
[8] A. B. Attya, "Wind enery penetration impact on grid frequency during normal operation and frequency deviations," Thesis for PhD, Electronic and Electrical Engineering, Technical University of Dramstadt, Darmstadt, Germany, 2014.
[9] D. G. Hart, D. Uy, V. Gharpure, D. Novosel, D. Karlsson, and M. Kaba, "PMUs – A new approach to power network monitoring," 2001.
[10] "Rate of Change of Frequency (RoCoF) Modification to the Grid Code," The Commission for Energy Regulation, Republic of Ireland, 2014.

Ayman Attya is a Research Associate in the Institute for Energy and Environment at the University of Strathclyde, UK. He received his BSc and MSc degrees of Electrical Power Engineering from Ain Shams University, Cairo, Egypt in 2005 and 2008 respectively. He was awarded the DAAD full PhD scholarship in 2010; thereupon he received the title of Doctor Engineer (Dr.-Ing.) from the Technical University of Darmstadt, Germany in 2014. He is a major investigator in wind integration research projects funded by the EU through the European Energy Research Alliance (EERA). His research interests are power systems stability and modelling, energy conversion, control systems design, and wind power.

Olimpo Anaya-Lara is a Reader in the Institute for Energy and Environment at the University of Strathclyde, UK. Dr. Anaya-Lara is a key participant to the Wind Integration Sub-Program of the European Energy Research Alliance (EERA) Joint Program Wind (JP Wind), leading Strathclyde contributions to this Sub-Program. He is CI of the EPSRC Supergen Wind Hub and member of the Management Core Team of the EPSRC Centre for Doctoral Training in Wind and Marine Energy Systems at Strathclyde. He was appointed to the post of Visiting Professor in Wind Energy at NTNU, Trondheim, Norway (2010-2011). His research interests are power electronic equipment, control systems design, and stability and control of power systems with increased wind energy penetration.